

1 **Blue OLEDs with narrow bandwidth using CF₃ substituted**
2 **bis((carbazol-9-yl)phenyl)amines as emitters: structural**
3 **regulation of linker between donor and acceptor in**
4 **chromophores**

5 Longzhi Zhu,^{a,b,c} Hongyang Zhang,^{b,c} Xiao Peng,^{a,*} Miao Zhang,^{b,c} Feifan Zhou,^a
6 Shuming Chen,^{d,*} Jun Song,^{a,*} Junle Qu^{a,e} and Wai-Yeung Wong^{b,c,*}

7 ^a Center for Biomedical Optics and Photonics (CBOP) & College of Physics and
8 Optoelectronic Engineering, Key Laboratory of Optoelectronic Devices and Systems,
9 Shenzhen University, Shenzhen 518060, P. R. China. Email: pengxiao_px@szu.edu.cn
10 (X. Peng); songjun@szu.edu.cn (J. Song)

11 ^b Department of Applied Biology and Chemical Technology and Research Institute for
12 Smart Energy, The Hong Kong Polytechnic University, Hung Hom, Kowloon, Hong
13 Kong, P. R. China. Email: wai-yeung.wong@polyu.edu.hk (W.-Y. Wong)

14 ^c The Hong Kong Polytechnic University Shenzhen Research Institute, Shenzhen 518057,
15 P. R. China.

16 ^d Department of Electrical and Electronic Engineering, Southern University of Science
17 and Technology, Shenzhen 518055, P. R. China. Email: chensm@sustech.edu.cn (S.
18 Chen)

19 ^e National Research Nuclear University MEPhI (Moscow Engineering Physics Institute),
20 115409, Moscow, Russian Federation

21

22 **Abstract**

23 Three new donor-acceptor (D-A) chromophores decorated with bis(trifluoromethyl)-
24 substituted phenyl group as acceptor and bis(4-(9*H*-carbazol-9-yl)phenyl)amine as donor
25 unit, namely 1,4-naphthyl-CF₃ (**1**), 1,5-naphthyl-CF₃ (**2**) and Ph-CF₃ (**3**), were designed
26 and synthesized. Their photophysical and electrochemical characteristics, and
27 corresponding theoretical calculations were investigated. They showed blue emissions
28 with high photoluminescence quantum yields (PLQY). Doped organic light-emitting
29 diodes (OLEDs) based on them were fabricated, which exhibited strong blue
30 electroluminescence with emission peaks at 453, 446 and 440 nm and full width at half
31 maximum (FWHM) of 69, 65 and 65 nm, respectively, Their Commission International
32 del'Eclairage (CIE) coordinates correspond to (0.169, 0.158), (0.176, 0.134) and (0.163,
33 0.099). Besides, the maximum current efficiencies (CEs) of 2.8, 5.0 and 4.9 cd A⁻¹; power
34 efficiencies (PEs) of 2.9, 5.4 and 5.2 lm W⁻¹; external quantum efficiencies (EQEs) of
35 2.3, 2.3 and 3.4% were achieved for 1,4-naphthyl-CF₃ (**1**), 1,5-naphthyl-CF₃ (**2**) and Ph-
36 CF₃ (**3**) doped devices D1, D2 and D3, respectively. This study clearly showed that the
37 optoelectronic properties of these organic small molecules can be regulated by rational
38 design of molecular structures, and their emission wavelengths could be finely tuned
39 within the blue region.

40

41 **Key words**

42 Blue OLEDs, Donor-acceptor structures, Narrow bandwidth, Structural regulation

43

44 **1. Introduction**

45 During the past decades, OLEDs has attracted intensive attention since the pioneering
46 work by Tang *et al* in 1987.[1] Efficient emitters for the three primary red, green and blue
47 colors have attained substantial developments and their optimized OLEDs have shown
48 remarkable advantages like high luminescent efficiency, large-area display, flexible panel
49 production, wide-viewing angle, low power consumption and so on.[2-5] Tuning the
50 OLED emission wavelength to the blue region especially the deep blue color has been of
51 particular significance because such light color finds useful applications in full-color
52 OLEDs displays and white light illumination sources.[6-8]

53 Blue emitters, especially deep blue emitters with CIE y coordinate value smaller than
54 0.1, are particularly scarce and challenging due to the high energy gap of the emitters.[9-
55 11] Although it is of great challenge, many efforts have been expended to achieve the
56 blue emission. For example, transition metal complexes as emitters that are used to afford
57 the blue phosphorescence, have drawn intense interest, because they can approach ideal
58 100% internal quantum efficiency by utilizing both singlet and triplet excitons.[12-14]
59 Other kinds of molecules, such as AIEgens,[15, 16] “hot exciton” fluorophores,[17, 18]
60 thermally activated delayed fluorescence (TADF) materials,[11, 19-24] hybridized local
61 and charge transfer (HLCT) materials,[25, 26] are also investigated to realize blue
62 emissions. However, the above-mentioned materials have some shortcomings which
63 limit their practical application. For example, phosphorescent metal complexes are

64 commonly air-/moisture- sensitive, environmentally toxic, and expensive. AIEgens, “hot
65 exciton” fluorophores, TADF and HLCT materials need the special skeletons with a
66 certain pattern of distributed HOMO and LUMO, causing the fine regulation of the
67 emission wavelength difficult. Therefore, it is still desirable to find alternative and
68 accessible ways to develop efficient, stable, pure- and deep-blue materials.

69 Organic small molecules as a kind of traditional chromophores have always attracted
70 many interests because of their merits in molecular diversity, mass production, tunable
71 energy gap, and low cost. Recently, donor-acceptor (D-A) type structure endowing the
72 materials with bipolar properties which can facilitate the hole/electron injection and
73 transport,[27-29] has been extensively investigated.[30] On the other hand, the
74 trifluoromethyl-related group has been demonstrated to be a good acceptor in the D-A
75 type blue materials,[31-34] and triarylamine is also a powerful and common donor for
76 constructing blue emitting materials due to its sufficiency in electron and high emission
77 efficiency.[35, 36] The functional material combining these two kinds of donor and
78 acceptor would be a good candidate for designing efficient deep blue emitters. The linker
79 between the donor and acceptor units also play an important role in the emission property
80 of emitters.[15, 37] Herein, we designed and synthesized three deep blue chromophores,
81 namely 1,4-naphthyl-CF₃ (**1**), 1,5-naphthyl-CF₃ (**2**) and Ph-CF₃ (**3**) (Scheme 1A), by
82 incorporating 2,4-bis(trifluoromethyl)-substituted phenyl group as acceptor, bis(4-(9H-
83 carbazol-9-yl)phenyl)amine as donor unit, and a different linker between the donor and
84 acceptor part. The OLEDs employing these emitters (**1-3**) as the dopants all exhibited the
85 pure blue luminescence with emission peak at 453, 446 and 440 nm; FWHM of 69, 65

86 and 65 nm; and CIE coordinates of (0.169, 0.158), (0.176, 0.134) and (0.163, 0.099),
87 respectively. This study clearly showed that the photoluminescence of **1-3** can be readily
88 regulated by molecular structural design, and particularly the emission wavelength of the
89 designed fluorophores can be finely tuned within the blue region.

90

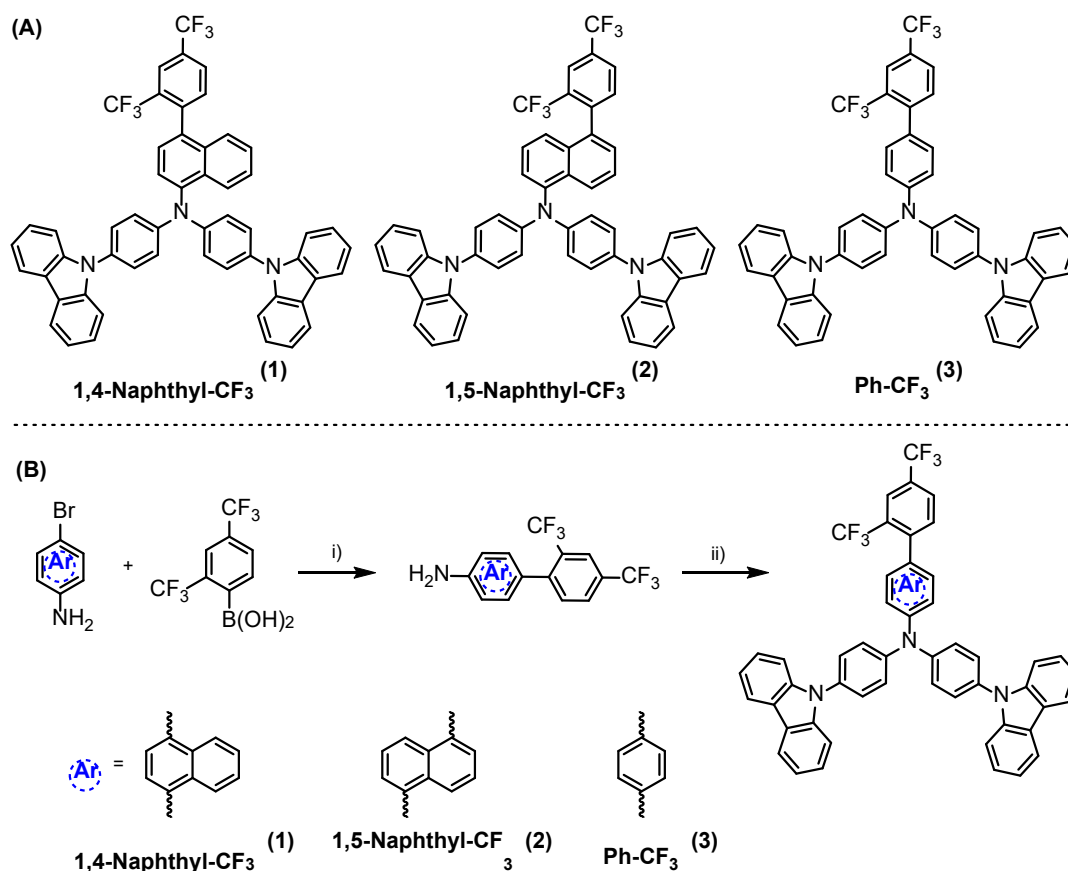
91 **2. Results and discussion**

92 2.1 Synthesis and characterization

93 The molecular structures of **1-3** are illustrated as shown in Scheme 1A, where the
94 differences of them are the central arylene linkage and the bonding sites. These structures
95 were successfully synthesized in 40-75% total yields via a two-step synthetic procedure
96 as described in Scheme 1B. The CF₃-substituted amine intermediates were prepared by
97 a Suzuki cross coupling reaction of (2,4-bis(trifluoromethyl)phenyl)boronic acid with the
98 corresponding bromo-amines, and the donor part was subsequently attached to it by a
99 Pd-catalyzed Buchwald–Hartwig reaction. The title compounds **1-3** were characterized
100 by NMR spectroscopy (¹H, ¹³C and ¹⁹F NMR) and high resolution mass spectrometry,
101 testifying the well-defined chemical structures and good purities. The detailed
102 procedures for the synthesis and characterization data are given in the supporting
103 information.

104 We tested the thermal stability of these compounds by the thermogravimetric analysis
105 (TGA) under a N₂ atmosphere. As shown in Figure S1, the decomposition temperature
106 (*T_d*) at 5% loss of the initial weight was 374, 391 and 405 °C for **1-3**, respectively,

107 exhibiting good thermal stabilities and demonstrating that these chromophores would be
108 sufficiently stable in the device fabrication process via evaporation and vapor deposition.



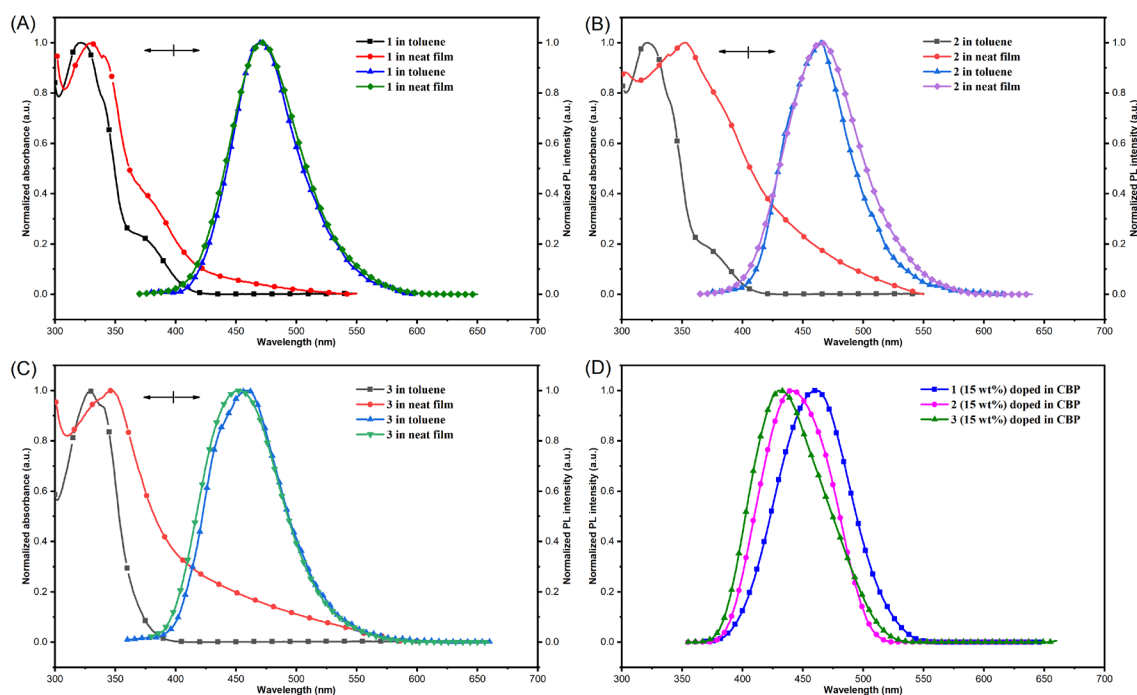
109

110 Scheme 1 Chemical structures (A) and synthetic routes (B) for 1,4-naphthyl-CF₃ (1), 1,5-
111 naphthyl-CF₃ (2), and Ph-CF₃ (3). Conditions: i) Pd(PPh₃)₄ (10 mol%), K₂CO₃ (2 equiv),
112 EtOH/H₂O/Toluene, N₂, 110 °C, 12 h; ii) 9-(4-bromophenyl)-9*H*-carbazole (2.5 equiv),
113 Pd₂(dba)₃ (5 mol%), ^tBu₃P-HBF₄ (10 mol%), ^tBuONa (3 equiv), Toluene, N₂, 120 °C, 12
114 h.

115 2.2 Photophysical and thermal properties

116 The photophysical properties of the three CF₃-substituted D-A chromophores were
117 characterized using UV-visible absorption and photoluminescence (PL) measurements,
118 and the results are presented and summarized as shown in Figure 1 and Table 1. The

119 maximum absorption peak in toluene solution appears at 321, 322 and 329 nm for **1-3**,
120 respectively, indicating a strong intramolecular π - π^* electronic transition. It is noted that
121 **1** and **2** shared similar absorption spectra in toluene, suggesting that the bonding site of
122 the central unit does not affect much of the electronic transition. However, in the neat
123 film state, the maximum absorption peak redshifted to 331, 352 and 347 nm for **1-3**,
124 respectively. The emission peak of the PL spectra at 469, 463 and 461 nm with a
125 relatively narrow FWHM of 63, 63 and 71 nm was recorded for **1-3** in toluene solution,
126 respectively. A slight blueshift in the emission spectra was observed when the central
127 motif was switched from naphthyl to phenyl group due to the decrease of the conjugation.
128 As shown in Figures 1A-C, compared to the solution state, the PL emission spectra in
129 neat film state were roughly the same. However, when they were doped in 4,4'-di(9H-
130 carbazol-9-yl)-1,1'-biphenyl (CBP), a blueshift was observed with the PL peaks of 459,
131 444 and 430 nm for **1-3** as shown in Figure 1D. As summarized in Table 1, they showed
132 photoluminescence quantum yield (PLQY) of 66.9, 36.3 and 84.9% in toluene for **1**, **2**
133 and **3**, respectively. However, in neat film state, the PLQY was reduced to 28.8, 11.2 and
134 34.8%, indicating that these emitters may suffer from a common aggregation-caused
135 quenching (ACQ) effect to some extent caused by the intermolecular π - π stacking. In
136 addition, the lifetime (τ) of 6.24, 5.61 and 3.12 ns in toluene was recorded. Accordingly,
137 we obtained the nonradiative decay rate constants (k_{nr}) and the radiative rate constants
138 (k_r) in solution. Compound **3** has the highest k_r and the lowest k_{nr} among the three
139 chromophores, as a result of the highest PLQY and a relatively shorter lifetime which
140 were observed.



141

142 Figure 1 The UV-vis absorption and PL spectra for **1** (A), **2** (B) and **3** (C) in toluene
 143 solution and neat film at 298 K. D: PL spectra for **1-3** measured in doped CBP film (15
 144 wt%).

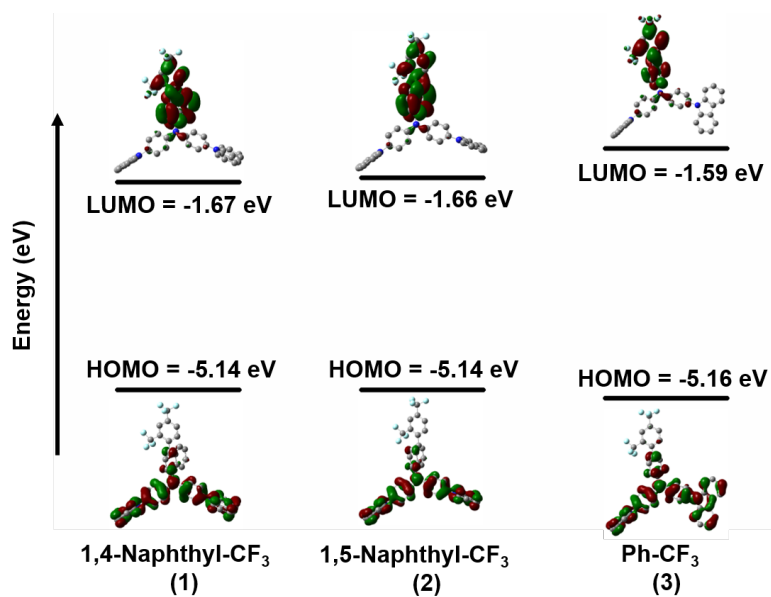
145 Table 1. Photophysical properties for **1-3**

Emitter	$\lambda_{\text{max}}^{\text{abs}}$ (^a / _b nm)	$\lambda_{\text{max}}^{\text{PL}}$ (^a / _b nm)	Φ^{em} (^a / _b %)	τ^{em} (ns) ^a	k_r/k_{nr} (10 ⁸ s ⁻¹) ^c	HOMO (^d / _e eV)	LUMO (^d / _f eV)
1	321/331	469/474	66.9/28.8	6.24	1.07/0.53	-5.14, -5.24	-1.67, -2.21
2	322/352	463/464	36.3/11.2	5.61	0.64/1.14	-5.14, -5.23	-1.66, -2.18
3	329/347	461/454	84.9/34.8	3.12	2.72/0.49	-5.16, -5.26	-1.59, -1.93

146 ^a Measured in toluene solution (10 μM). ^b Measured in neat film. ^c Calculated by the
 147 equation $\Phi^{\text{em}} = k_r \tau^{\text{em}} = k_r / (k_r + k_{\text{nr}})$. ^d Energy levels estimated from the DFT calculation
 148 results. ^e Energy levels estimated from CV curves. ^f Calculated from the equation LUMO
 149 = HOMO + E_g^{opt} , where E_g^{opt} is the optical energy band gap estimated from UV-vis
 150 spectra.

151 2.3 Theoretical calculations

152 To better understand the optoelectronic properties of these D-A structures at the
153 molecular level, we performed the density functional theory (DFT) calculations using
154 Gaussian 09 suite of programs at the B3LYP/6-31G(d) level.[38] The distributions and
155 energy levels of the highest occupied molecular orbital (HOMO) and lowest unoccupied
156 molecular orbital (LUMO) for **1-3** are shown in Figure 2 and Table 1. All the three
157 compounds were observed with highly twisted conformation from the optimized
158 geometry. As shown in Figure 2, the HOMO levels of these structures were mainly
159 located on the bis-carbazolyl amine unit and partly on the adjacent phenyl group, while
160 the LUMO levels were mostly distributed on the CF₃-substituted phenyl group and its
161 adjacent phenyl or naphthyl group. Thus, the HOMO and LUMO distributions
162 overlapped slightly on the middle benzene unit between CF₃-substituted phenyl group
163 and bis-carbazolyl amine moiety. The partial overlap of the frontier orbitals may promote
164 the radiative decay and result in efficient luminescence.[39] Furthermore, **1** and **2** share
165 a very similar feature both in the HOMO and LUMO distributions and levels from DFT
166 estimation, which may be responsible for the closely similar UV-vis absorption spectra
167 observed in toluene solution (Figures 1A-B). In addition, the energy gap between HOMO
168 and LUMO of **3** (3.57 eV) is larger than that of **1** (3.47 eV) and **2** (3.48 eV), which is
169 consistent with the higher energy emission of **3** in the PL spectrum (Figure 1).



170

171 Figure 2 HOMO and LUMO energy levels and distributions for the optimized geometry
 172 of **1-3**.

173 2.4 Electrochemical properties

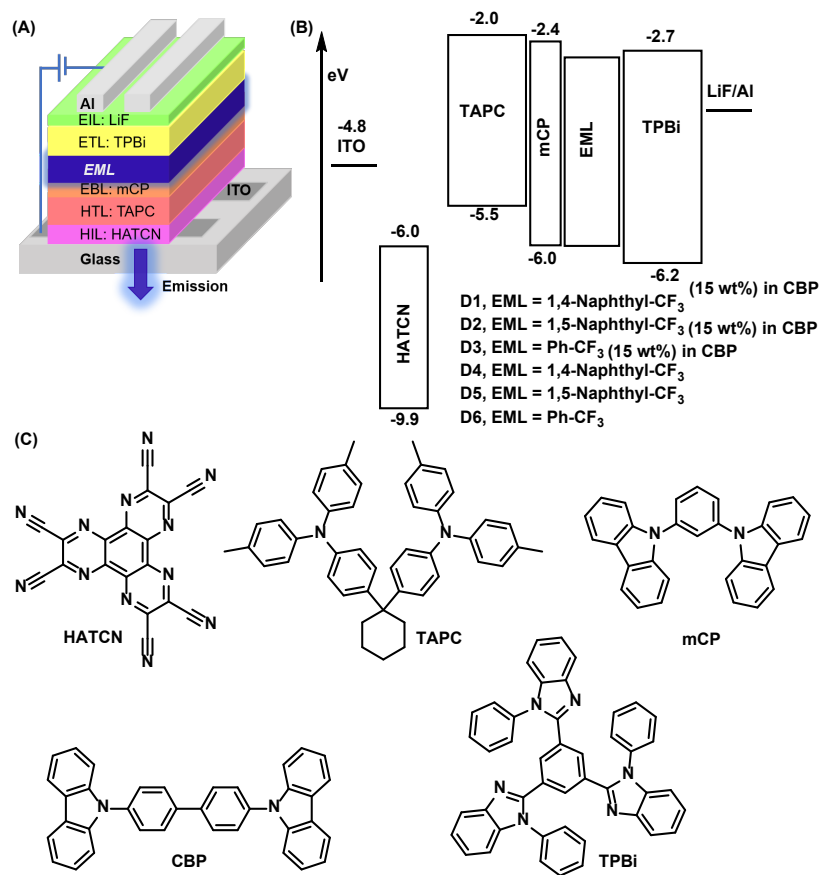
174 The cyclic voltammetry (CV) has been performed to investigate the electrochemical
 175 properties of the three fluorophores with ferrocene as the internal standard under a N₂
 176 atmosphere. From Figure S2, reversible oxidation waves were observed for these D-A
 177 chromophores with an oxidation peak at 1.27, 1.33 and 1.34 V, which can be ascribed to
 178 the oxidation of the bis(4-(9*H*-carbazol-9-yl)phenyl)amine motifs. The HOMO was then
 179 estimated from the electrochemically determined oxidation potential versus that of
 180 ferrocene, and the LUMO was estimated from the electrochemically determined HOMO
 181 plus the optical band gap evaluated from the onset wavelength of UV-vis absorption. As
 182 shown in Table 1, the HOMO/LUMO energy levels for **1-3** were -5.24/-2.21, -5.23/-2.18,
 183 -5.26/-1.93 eV, respectively, which favorably agrees with the results estimated from the
 184 DFT calculations.

185 2.5 Electroluminescence properties

186 In view of the excellent blue emitting properties of these CF₃-substituted D-A
187 chromophores, we used **1-3** as the emitters to study their electroluminescence (EL)
188 performance, and the associated doped OLED devices (D1-D3) were fabricated. Thermal
189 vacuum deposition was chosen to fabricate the devices due to the good thermal stabilities
190 of these chromophores. The device configuration consists of the following layers:
191 ITO/HATCN (20 nm)/TAPC (40 nm)/mCP (5 nm)/EML (20 nm)/TPBi (40 nm)/LiF (1
192 nm)/Al (100 nm) as described in Figure 3A and B,[40] where ITO (indium tin oxide) and
193 Al (aluminum) worked as the anode and cathode, HATCN (dipyrazino[2,3-*f*:2',3'-
194 *h*]quinoxaline-2,3,6,7,10,11-hexacarbonitrile) and LiF (lithium fluoride) as the hole and
195 electron injection layers (HIL/EIL), 4,4'-(cyclohexane-1,1-diyl)bis(*N,N*-di-*p*-
196 tolylaniline) (TAPC) as the hole transporting layer (HTL), 1,3-di(9*H*-carbazol-9-
197 yl)benzene (mCP) as the electron blocking layer (EBL)[41] and 1,3,5-tris(1-phenyl-1*H*-
198 benzo[*d*]imidazol-2-yl)benzene (TPBi) as the electron transporting layer (ETL). Here the
199 host is 4,4'-di(9*H*-carbazol-9-yl)-1,1'-biphenyl (CBP). The electroluminescence data are
200 presented and summarized in Figure 4 and Table 2.

201 As shown in Figure 4A, when a proper voltage was applied, the three devices D1-D3
202 doped with CBP (15 wt%) exhibited blue electroluminescence, with the maximum peak
203 of EL spectra at 453, 446 and 440 nm and a relatively narrow FWHM of 69, 65, 65 nm,
204 respectively. These EL peaks were comparable to those in the PL spectra at film state
205 with the doping concentration of 15 wt% in CBP (Figure 1D), which were 459, 444 and
206 430 nm for **1-3**, respectively. As depicted in Table 2 and Figure S8, these devices D1-D3

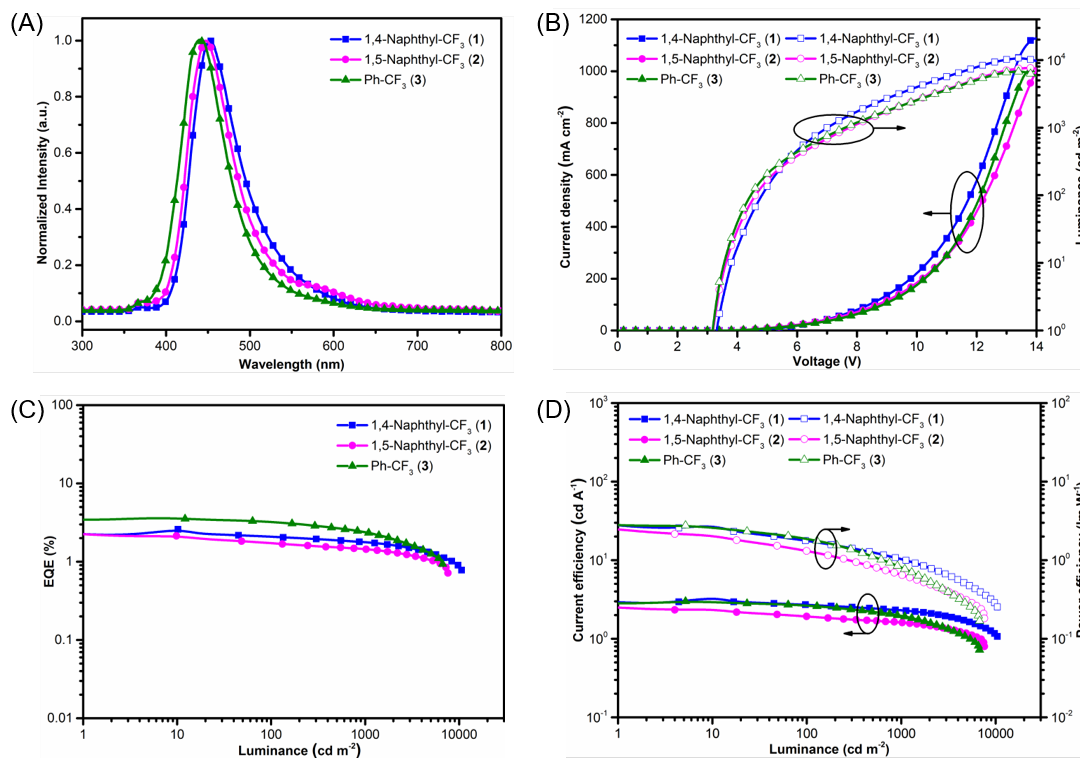
207 exhibited CIE chromaticity coordinates of (0.169, 0.158), (0.176, 0.134) and (0.163,
208 0.099), respectively, exhibiting strong blue emissions. Especially, the D3 displays the
209 deep blue luminescence with a CIE of (0.163, 0.099), in which the CIE y value is smaller
210 than 0.1. These blue OLEDs showed low turn-on voltages (V_{on} , at a luminance of 1 cd
211 m^{-2}) at the range of 3.2-3.3 V as given from Figure 4B.[42] The maximum luminance
212 (L_{max}) of devices D1-D3 can reach 10640, 7621 and 6749 $cd m^{-2}$, respectively, which is
213 superior to other blue OLEDs emitting the similar light.[43] Figures 4C-D show the
214 EQE- L and CE & PE- L curves, in which maximum CEs of 2.8, 5.0, and 4.9 $cd A^{-1}$; PEs
215 of 2.9, 5.4, and 5.2 $lm W^{-1}$ were realized for **1-3** based devices D1, D2 and D3,
216 respectively. The device D3 gave the highest quantum efficiency among the three doped
217 blue OLEDs with a peak EQE of 3.4%, which is consistent with the trend of PLQY.
218 Switching the central structure from phenyl to naphthyl led to the decrease of the EQE
219 to 2.3% probably due to the more vibrational quenching caused by the increased
220 conjugation structure. By using the same device architecture, the nondoped OLED
221 devices D4-D6 based on **1-3** were also investigated (Table 2 and Figure S7). Compared
222 with the devices doped with CBP, the EL spectra of these nondoped devices were slightly
223 redshifted. Remarkably, similar EQEs in nondoped devices were achieved compared to
224 that of the doped devices, indicating that this family of chromophores may have the
225 potential to be used as the host materials.



226

227 Figure 3 The architecture (A) and energy levels (B) of the devices; the chemical

228 structures of the materials used in the devices (C).



229

230 Figure 4 The performance of the three OLED devices. The EL spectra (A), current
 231 density-voltage-luminance (J - V - L) curves (B), EQE-luminance (C), and CE and PE vs
 232 luminance (D) for the doped devices D1-D3, respectively.

233 Table 2. The EL performance of doped (D1-D3) and nondoped (D4-D6) OLEDs devices

Device	$\lambda_{\text{max}}^{\text{EL}}$ (nm)	FWHM (nm)	EQE ^a (%)	CE ^b (cd A ⁻¹)	PE ^b (lm W ⁻¹)	L_{max} (cd m ⁻²)	V_{on} (V) ^c	CIE (x, y)
D1	453	69	2.3/2.1/1.8	2.8	2.9	10640	3.3	0.169, 0.158
D2	446	65	2.3/1.7/1.4	5.0	5.4	7621	3.2	0.176, 0.134
D3	440	65	3.4/3.2/2.4	4.9	5.2	6749	3.2	0.163, 0.099
D4	457	78	2.4/2.6/2.4	4.1	2.7	13080	4.4	0.166, 0.198
D5	447	75	2.2/2.2/2.0	3.0	2.3	7424	4.0	0.170, 0.163
D6	440	66	2.5/3.1/2.9	3.3	1.9	6659	4.9	0.167, 0.130

234 ^a Efficiency recorded at 1/100/1000 cd m⁻². ^b Maximum efficiency. ^c Turn-on voltage
 235 recorded at a luminance of 1 cd m⁻².

236 In order to further investigate the effect of the central linkage between the D and A
 237 parts, we prepared a compound (quinoline-CF₃, **4**) with quinoline as the central linker to
 238 connect the same D and A moieties. Compound **4** showed a photoluminescence peak at
 239 516 nm and absorption peaks at 320 and 405 nm in toluene (Figure S10A). A doped
 240 OLED by using **4** as the emitter was also fabricated under the same architecture of D1 as
 241 depicted in Figure 3A, which emitted a blue-green light with a maximum EL peak at 517
 242 nm and the CIE coordinate of (0.269, 0.497) (Figure S10E and S11). Introduction of *N*-
 243 heterocyclic quinoline motif as the central linker can significantly stabilize the LUMO
 244 level (-1.94 eV),[44] leading to a bathochromic shift both in solution PL and EL from the

245 OLED. The OLEDs based on our developed chromophores clearly demonstrate that the
246 emission wavelength within the blue region could be finely tuned by changing the linker
247 and bonding site. We believe that better blue emitters can be easily realized by combining
248 the adopted molecular design strategy with other design strategies, such as by taking
249 advantages of harvesting both singlet and triplet excitons.

250

251 **3 Conclusion**

252 In conclusion, we designed and synthesized three new D-A type CF₃-substituted
253 bis((carbazol-9-yl)phenyl)amines by regulating the central motif, and their
254 optoelectronic properties have been fully investigated. All the three emitters are
255 demonstrated to exhibit strong blue light. Especially, the OLED device D3 using Ph-CF₃
256 (**3**) as the emitter exhibited a pure deep blue luminescence with the peak at 440 nm,
257 FWHM of 65 nm and CIE coordinate of (0.163, 0.099), in which the CIE y coordinate
258 value is notably smaller than 0.1. Our study here presents a viable organic synthesis
259 strategy for achieving efficient deep blue emitters. By simplifying the conjugation or
260 altering the bonding site of the linker, we realized the fine regulation of the emission
261 wavelength within the blue region.

262

263 **Conflict of interest**

264 We declare that we do not have any commercial or associative interest that represents a
265 conflict of interest in connection with the work.

266

267 **Acknowledgements**

268 This work has been partially supported by the National Natural Science Foundation of
269 China (61620106016/61835009/61775145/31771584/52073242); Guangdong Province
270 Key Area R&D Program (2019B110233004); Shenzhen Basic Research Project
271 (JCYJ20170818100153423); Natural Science Foundation of SZU (No. 2017000193).
272 W.-Y.W. would like to thank the Science, Technology and Innovation Committee of
273 Shenzhen Municipality (JCYJ20180507183413211); the Hong Kong Research Grants
274 Council (PolyU 153058/19P); Hong Kong Polytechnic University (1-ZE1C), Research
275 Institute for Smart Energy (RISE) and the Endowed Professorship in Energy from Ms.
276 Clarea Au (847S) for financial support.

277

278 **References**

- 279 [1] Tang CW, VanSlyke SA. Organic Electroluminescent Diodes. *Appl Phys Lett*
280 1987;51:913-5.
- 281 [2] Hong G, Gan X, Leonhardt C, Zhang Z, Seibert J, Busch JM, et al. A Brief History
282 of OLEDs-Emitter Development and Industry Milestones. *Adv Mater* 2021;33:e2005630.
- 283 [3] Wei Q, Fei N, Islam A, Lei T, Hong L, Peng R, et al. Small-Molecule Emitters with
284 High Quantum Efficiency: Mechanisms, Structures, and Applications in OLED Devices.
285 *Adv Opt Mater* 2018;6:1800512.
- 286 [4] Zhu XH, Peng J, Cao Y, Roncali J. Solution-Processable Single-Material Molecular
287 Emitters for Organic Light-Emitting Devices. *Chem Soc Rev* 2011;40:3509-24.
- 288 [5] Grimsdale AC, Leok Chan K, Martin RE, Jokisz PG, Holmes AB. Synthesis of Light-

289 Emitting Conjugated Polymers for Applications in Electroluminescent Devices. *Chem*
290 *Rev* 2009;109:897-1091.

291 [6] Im Y, Byun SY, Kim JH, Lee DR, Oh CS, Yook KS, et al. Recent Progress in High-
292 Efficiency Blue-Light-Emitting Materials for Organic Light-Emitting Diodes. *Adv Funct*
293 *Mater* 2017;27:1603007.

294 [7] Reineke S, Lindner F, Schwartz G, Seidler N, Walzer K, Lussem B, et al. White
295 Organic Light-Emitting Diodes with Fluorescent Tube Efficiency. *Nature* 2009;459:234-
296 8.

297 [8] Yook KS, Lee JY. Organic Materials for Deep Blue Phosphorescent Organic Light-
298 Emitting Diodes. *Adv Mater* 2012;24:3169-90.

299 [9] Zhu M, Yang C. Blue Fluorescent Emitters: Design Tactics and Applications in
300 Organic Light-Emitting Diodes. *Chem Soc Rev* 2013;42:4963-76.

301 [10] Lee JH, Chen CH, Lee PH, Lin HY, Leung MK, Chiu TL, et al. Blue Organic Light-
302 Emitting Diodes: Current Status, Challenges, and Future Outlook. *J Mater Chem C*
303 2019;7:5874-88.

304 [11] Godumala M, Choi S, Cho MJ, Choi DH. Thermally Activated Delayed
305 Fluorescence Blue Dopants and Hosts: From the Design Strategy to Organic Light-
306 Emitting Diode Applications. *J Mater Chem C* 2016;4:11355-81.

307 [12] Jung M, Lee KH, Lee JY, Kim T. A Bipolar Host Based High Triplet Energy
308 Electroplex for an over 10 000 h Lifetime in Pure Blue Phosphorescent Organic Light-
309 Emitting Diodes. *Mater Horiz* 2020;7:559-65.

310 [13] Yang X, Zhou G, Wong WY. Functionalization of Phosphorescent Emitters and
311 Their Host Materials by Main-Group Elements for Phosphorescent Organic Light-
312 Emitting Devices. *Chem Soc Rev* 2015;44:8484-575.

313 [14] Li G, Zhao X, Fleetham T, Chen Q, Zhan F, Zheng J, et al. Tetradentate Platinum(II)
314 Complexes for Highly Efficient Phosphorescent Emitters and Sky Blue OLEDs. *Chem*
315 *Mater* 2019;32:537-48.

316 [15] Chen L, Lin G, Peng H, Ding S, Luo W, Hu R, et al. Sky-Blue Nondoped OLEDs
317 Based on New Aiegens: Ultrahigh Brightness, Remarkable Efficiency and Low

318 Efficiency Roll-Off. *Mater Chem Front* 2017;1:176-80.

319 [16] Fei N, Wei Q, Cao L, Bai Y, Ji H, Peng R, et al. A Symmetric Nonpolar Blue Aiegen
320 as Nondoped Fluorescent OLED Emitter with Low Efficiency Roll-Off. *Org Electron*
321 2020;78:105574.

322 [17] Xu Y, Liang X, Zhou X, Yuan P, Zhou J, Wang C, et al. Highly Efficient Blue
323 Fluorescent OLEDs Based on Upper Level Triplet-Singlet Intersystem Crossing. *Adv*
324 *Mater* 2019;31:e1807388.

325 [18] Yang J, Guo Q, Wang J, Ren Z, Chen J, Peng Q, et al. Rational Molecular Design
326 for Efficient Exciton Harvesting, and Deep-Blue OLED Application. *Adv Opt Mater*
327 2018;6:1800342.

328 [19] Hatakeyama T, Shiren K, Nakajima K, Nomura S, Nakatsuka S, Kinoshita K, et al.
329 Ultrapure Blue Thermally Activated Delayed Fluorescence Molecules: Efficient HOMO-
330 LUMO Separation by the Multiple Resonance Effect. *Adv Mater* 2016;28:2777-81.

331 [20] Chan C-Y, Tanaka M, Lee Y-T, Wong Y-W, Nakanotani H, Hatakeyama T, et al.
332 Stable Pure-Blue Hyperfluorescence Organic Light-Emitting Diodes with High-
333 Efficiency and Narrow Emission. *Nat Photonics* 2021;15:203-7.

334 [21] Hirata S, Sakai Y, Masui K, Tanaka H, Lee SY, Nomura H, et al. Highly Efficient
335 Blue Electroluminescence Based on Thermally Activated Delayed Fluorescence. *Nat*
336 *Mater* 2015;14:330-6.

337 [22] Zhu X-D, Tian Q-S, Zheng Q, Tao X-C, Yuan Y, Yu Y-J, et al. A Sky-Blue Thermally
338 Activated Delayed Fluorescence Emitter Based on Multimodified Carbazole Donor for
339 Efficient Organic Light-Emitting Diodes. *Org Electron* 2019;68:113-20.

340 [23] Serevičius T, Skaisgiris R, Fiodorova I, Steckis V, Dodonova J, Banevičius D, et al.
341 Achieving Efficient Deep-Blue TADF in Carbazole-Pyrimidine Compounds. *Org*
342 *Electron* 2020;82:105723.

343 [24] Luo Y, Li S, Zhao Y, Li C, Pang Z, Huang Y, et al. An Ultraviolet Thermally
344 Activated Delayed Fluorescence OLED with Total External Quantum Efficiency over 9.
345 *Adv Mater* 2020;32:e2001248.

346 [25] Lv X, Sun M, Xu L, Wang R, Zhou H, Pan Y, et al. Highly Efficient Non-Doped

347 Blue Fluorescent OLEDs with Low Efficiency Roll-Off Based on Hybridized Local and
348 Charge Transfer Excited State Emitters. *Chem Sci* 2020;11:5058-65.

349 [26] Kumar Konidena R, Justin Thomas KR, Kumar Dubey D, Sahoo S, Jou JH. A New
350 Molecular Design Based on Hybridized Local and Charge Transfer Fluorescence for
351 Highly Efficient (>6%) Deep-Blue Organic Light Emitting Diodes. *Chem Commun*
352 2017;53:11802-5.

353 [27] Duan L, Qiao J, Sun Y, Qiu Y. Strategies to Design Bipolar Small Molecules for
354 OLEDs: Donor-Acceptor Structure and Non-Donor-Acceptor Structure. *Adv Mater*
355 2011;23:1137-44.

356 [28] Jiang J, Hu D, Hanif M, Li X, Su S, Xie Z, et al. Twist Angle and Rotation Freedom
357 Effects on Luminescent Donor-Acceptor Materials: Crystal Structures, Photophysical
358 Properties, and OLED Application. *Adv Opt Mater* 2016;4:2109-18.

359 [29] Li Z, Li C, Xu Y, Xie N, Jiao X, Wang Y. Nonsymmetrical Connection of Two
360 Identical Building Blocks: Constructing Donor-Acceptor Molecules as Deep Blue
361 Emitting Materials for Efficient Organic Emitting Diodes. *J Phys Chem Lett*
362 2019;10:842-7.

363 [30] Yuan Y, Chen J-X, Lu F, Tong Q-X, Yang Q-D, Mo H-W, et al. Bipolar
364 Phenanthroimidazole Derivatives Containing Bulky Polyaromatic Hydrocarbons for
365 Nondoped Blue Electroluminescence Devices with High Efficiency and Low Efficiency
366 Roll-Off. *Chem Mater* 2013;25:4957-65.

367 [31] Yi CL, Ko CL, Yeh TC, Chen CY, Chen YS, Chen DG, et al. Harnessing a New Co-
368 Host System and Low Concentration of New TADF Emitters Equipped with
369 Trifluoromethyl- and Cyano-Substituted Benzene as Core for High-Efficiency Blue
370 OLEDs. *ACS Appl Mater Interfaces* 2020;12:2724-32.

371 [32] Liang X, Han H-B, Yan Z-P, Liu L, Zheng Y-X, Meng H, et al. Versatile
372 Functionalization of Trifluoromethyl Based Deep Blue Thermally Activated Delayed
373 Fluorescence Materials for Organic Light Emitting Diodes. *New J Chem* 2018;42:4317-
374 23.

375 [33] Mei L, Hu J, Cao X, Wang F, Zheng C, Tao Y, et al. The Inductive-Effect of Electron

376 Withdrawing Trifluoromethyl for Thermally Activated Delayed Fluorescence: Tunable
377 Emission from Tetra- to Penta-Carbazole in Solution Processed Blue OLEDs. *Chem*
378 *Commun* 2015;51:13024-7.

379 [34] Yuan W, Zhang M, Zhang X, Cao X, Sun N, Wan S, et al. The Electron Inductive
380 Effect of Cf₃ on Penta-Carbazole Containing Blue Emitters: Trade-Off between Color
381 Purity and Luminescent Efficiency in TADF OLEDs. *Dyes Pigments* 2018;159:151-7.

382 [35] Tagare J, Yadav RAK, Swayamprabha SS, Dubey DK, Jou J-H, Vaidyanathan S.
383 Efficient Solution-Processed Deep-Blue C_{iey} ∈ (0.05) and Pure-White C_{ieX,Y} ∈
384 (0.34, 0.32) Organic Light-Emitting Diodes: Experimental and Theoretical Investigation.
385 *J Mater Chem C* 2021;9:4935-47.

386 [36] Wang J, Liu K, Ma L, Zhan X. Triarylamine: Versatile Platform for Organic, Dye-
387 Sensitized, and Perovskite Solar Cells. *Chem Rev* 2016;116:14675-725.

388 [37] Tao Y, Wang Q, Yang C, Zhong C, Zhang K, Qin J, et al. Tuning the Optoelectronic
389 Properties of Carbazole/Oxadiazole Hybrids through Linkage Modes: Hosts for Highly
390 Efficient Green Electrophosphorescence. *Adv Funct Mater* 2010;20:304-11.

391 [38] Frisch MJ, Trucks GW, Schlegel HB, Scuseria GE, Robb MA, Cheeseman JR, et al.
392 Gaussian 09. Wallingford, CT2009.

393 [39] Zhang Y, Chen Z, Song J, He J, Wang X, Wu J, et al. Rational Design of High
394 Efficiency Green to Deep Red/near-Infrared Emitting Materials Based on Isomeric
395 Donor-Acceptor Chromophores. *J Mater Chem C* 2019;7:1880-7.

396 [40] Chen Z, Zhang H, Wen D, Wu W, Zeng Q, Chen S, et al. A Simple and Efficient
397 Approach toward Deep-Red to near-Infrared-Emitting Iridium(III) Complexes for
398 Organic Light-Emitting Diodes with External Quantum Efficiencies of over 10%. *Chem*
399 *Sci* 2020;11:2342-9.

400 [41] Udagawa K, Sasabe H, Cai C, Kido J. Low-Driving-Voltage Blue Phosphorescent
401 Organic Light-Emitting Devices with External Quantum Efficiency of 30%. *Adv Mater*
402 2014;26:5062-6.

403 [42] Tagare J, Boddula R, Yadav RAK, Dubey DK, Jou J-H, Patel S, et al. Novel
404 Imidazole-Alkyl Spacer-Carbazole Based Fluorophores for Deep-Blue Organic Light

405 Emitting Diodes: Experimental and Theoretical Investigation. *Dyes Pigments*
406 2021;185:108853.

407 [43] Jia WL, Feng XD, Bai DR, Lu ZH, Wang S, Vamvounis G. Mes₂B(*p*-4,4'-Biphenyl-
408 Nph(1-Naphthyl)): A Multifunctional Molecule for Electroluminescent Devices. *Chem*
409 *Mater* 2005;17:164-70.

410 [44] Park Y, Lee J-H, Jung DH, Liu S-H, Lin Y-H, Chen L-Y, et al. An Aromatic Imine
411 Group Enhances the El Efficiency and Carrier Transport Properties of Highly Efficient
412 Blue Emitter for OLEDs. *J Mater Chem* 2010;20:5930–6.

413